Ion Cyclotron Waves in Field-aligned Solar Wind Turbulence

Daniele Telloni[1] , Francesco Carbone[2] , Roberto Bruno[3] , Gary P. Zank[4,5] , Luca Sorriso-Valvo[6,7] , and Salvatore Mancuso[1]

[1] National Institute for Astrophysics—Astrophysical Observatory of Torino, Via Osservatorio 20, I-10025 Pino Torinese, Italy; daniele.telloni@inaf.it
[2] National Research Council—Institute of Atmospheric Pollution Research, c/o University of Calabria, I-87036 Rende, Italy
[3] National Institute for Astrophysics—Institute for Space Astrophysics and Planetology, Via del Fosso del Cavaliere 100, I-00133 Roma, Italy
[4] University of Alabama, Center for Space Plasma and Aeronomic Research, Huntsville, AL 35805, USA
[5] University of Alabama, Department of Space Science, Huntsville, AL 35805, USA
[6] Escuela Politécnica Nacional, Departamento de Física, Ladron de Guevera E11-253, Quito 170517, Ecuador
[7] National Research Council—Institute for the Science and Technology of Plasmas, Ponte P. Bucci Cubo 31C, I-87036 Rende, Italy

Abstract

The nature of the solar wind parallel fluctuations is investigated in this Letter by using magnetic helicity to characterize their polarization state at proton scales. Our aim is to assess the role of the proton cyclotron instability as a mechanism for generating ion cyclotron waves (ICWs) in solar wind turbulence. The wave polarization is found to depend strongly on the proton temperature anisotropy and on the power level of magnetic fluctuations at fluid scales. The results indicate a clear link between fluid and kinetic scales in the solar wind turbulence, allowing for a picture in which the resonant dissipation of high-frequency Alfvén waves heats protons in a direction perpendicular to the magnetic field, increasing their temperature anisotropy. The velocity distribution thus becomes unstable to the proton cyclotron instability, which then drives the local generation of ICWs in the solar wind.

1. Introduction

Ion cyclotron waves (ICWs) are left-handed polarized waves, with a nearly magnetic field-aligned wavevector and frequencies near the proton gyrofrequency $\Omega_p = qB/(m_p c)$, where q is the proton electric charge, B the local magnetic field intensity, m_p the proton rest mass, and c the speed of light. Evidence for their existence has been found both in the corona and the solar wind, where ICWs are considered to play an important role in plasma heating (see the review by Marsch 2006 and references therein). Remote-sensing observations of polar coronal holes, where the fast wind is accelerated, have revealed highly anisotropic heavy-ion velocity distribution functions (VDFs) in the corona (see reviews by Antonucci 2006; Kohl et al. 2006; Antonucci et al. 2012), with an apparent preferential energy deposition perpendicular to the magnetic field. This has been interpreted as a most clear signature of ion cyclotron resonance scattering by high-frequency Alfvén waves (Kohl et al. 1998; Cranmer et al. 1999). Similarly, in situ measurements of the proton temperature anisotropy, $T_\perp/T_\parallel > 1$, in high-speed streams (Marsch et al. 1982), are strongly correlated with enhancements in the transverse wave power spectrum at frequencies $\omega \lesssim \Omega_p$ (Bourouaine et al. 2010), which also suggests that ICWs could be driven by a proton temperature instability. The statistical study performed in the solar wind by Bale et al. (2009) provided strong evidence for enhanced magnetic fluctuations along the temperature anisotropy thresholds of the mirror, proton oblique firehose, and ion cyclotron instabilities, thus suggesting that these instabilities are at work in generating unstable modes. Furthermore, He et al. (2015) found that, along with the resonant interaction with left-handed Alfvén cyclotron waves (which heats the protons in a direction perpendicular to the magnetic field), kinetic Alfvén wave turbulence also efficiently dissipates, through proton Landau damping, energy

at frequencies near the proton gyrofrequency, resulting in a preferential parallel proton heating.

Direct observations of ICWs in the solar wind were first reported by Jian et al. (2009, 2010) as sporadic circularly polarized transverse wave packets, with frequencies close to Ω_p, propagating mainly in a direction parallel to the background magnetic field. Evidence that ICWs are ubiquitous in the solar wind turbulence was, however, provided later on by He et al. (2011) and Podesta & Gary (2011), who used the normalized magnetic helicity σ_m as an important diagnostic in studying the polarization state of various wave modes. They analyzed the distribution of normalized magnetic helicity as a function of the angle θ_{VB} between the solar wind velocity and local mean magnetic field vectors, identifying a population of fluctuations with $\sigma_m < 0$ at proton scales and small pitch angles with B, which has been interpreted as parallel-propagating left-handed polarized ICWs. However, the nature of the fluctuations within the ion-kinetic range clearly depends on the type of wind. ICWs are indeed gradually depleted if one considers first the fast and then the slow wind, as first noticed by Bruno & Telloni (2015). This suggests that the Alfvénicity and the amplitude of the fluctuations at fluid scales, rather than the wind speed, are crucial parameters in regulating the ion cyclotron signature. Telloni et al. (2015) then showed, by exploiting the radial alignment of the Messenger and Wind s/c, that ICWs tend to lower frequency as the wind expands, following the radial evolution of the proton gyrofrequency, evidently pointing to the strong relation of these wave modes with Ω_p. Both these observational results suggest that the ion cyclotron resonance is the most likely mechanism for the dissipation of energy transferred through the inertial range to heat the proton component of the solar wind plasma. Finally, Telloni & Bruno (2016) reported that ICWs occupy a region in the plasma beta-temperature anisotropy $\beta_\parallel - T_\perp/T_\parallel$ plane in which they are expected to become unstable for the proton

cyclotron instability, providing robust hints that the nature of the high-frequency magnetic fluctuations is correlated with the status of MHD turbulence. They argued that the existence of ICWs at ion-kinetic scales might be related to the presence of large-amplitude high-frequency Alfvén waves (ruled by the turbulent cascade of strong large-scale Alfvénic fluctuations), which would resonantly interact with protons around Ω_p causing an increase in the temperature anisotropy. This in turn would cause the proton velocity distribution to exceed the proton cyclotron instability threshold. In order to restore the VDFs toward an isotropic Maxwellian distribution, ICWs would be generated at frequencies near the proton gyrofrequencies, thereby releasing the energy excess built up in the anisotropic VDF (Hellinger et al. 2006). This conclusion was confirmed by subsequent statistical studies (Woodham et al. 2018; Zhao et al. 2019). These analyses, however, suffer from the impossibility of correctly separating contributions to magnetic helicity from fluctuations propagating in directions parallel and perpendicular to the local mean magnetic field, thus potentially mixing information derived from wave modes of different character.

To directly probe ICWs, the results from a systematic search for field-aligned solar wind time intervals that would be populated mostly by $k_\parallel$ fluctuations are presented in this Letter. The σ_m value of the coherent peak observed in the corresponding normalized magnetic helicity spectra around the proton gyrofrequency in the spacecraft frame $\Omega_{p,\mathrm{SC}} = \Omega_p \cdot V_{\mathrm{SW}}/V_{\mathrm{A}}$ (He et al. 2011, where V_{SW} and V_{A} are the solar wind and Alfvén speeds, respectively), which is a clear signature of the presence of parallel-propagating ICWs, is studied in correlation with kinetic and fluid parameters, such as the temperature anisotropy $T_\perp/T_\parallel$, the parallel proton plasma $\beta_\parallel$, and the power level of the magnetic fluctuations within the inertial range. This will illustrate the coupling of fluid and kinetic scales and allow us to understand how energy is released in the dissipation range, providing a definitive and comprehensive view of the kinetic processes underlying the generation of the ICWs in solar wind turbulence.

The layout of this Letter is as follows: a description of the data selection is given in Section 2, the analysis results are presented in Section 3, followed by some discussion and concluding remarks in Section 4.

2. Data Selection

To correlate the polarization of parallel-propagating magnetic fluctuations at $\omega \sim \Omega_{p,\mathrm{SC}}$ with the fluid properties of the solar wind turbulence, a through survey of time intervals robustly providing $k_\parallel$ sampling has been accomplished by using 12 yr worth of solar wind measurements acquired by the *Wind* spacecraft between 2005 and 2016. In particular, we use high-resolution 11 Hz magnetic field data from the Magnetic Field Investigation magnetometer (Lepping et al. 1995), and 92 s resolution ion moments, including the proton bulk speed V, density n_p, and temperature perpendicular $T_\perp$ and parallel $T_\parallel$ to the magnetic field direction from the Solar Wind Experiment instrument (Ogilvie et al. 1995).

The selection of the field-aligned time intervals is based on the following requirements. The pitch angle has to be small ($\theta_{VB} < 15°$) at all scales and for the whole data set, to ensure that we sample only quasi-parallel-propagating magnetic fluctuations. The time intervals have to be at least 1 hr long, to allow the investigation to range from kinetic to fluid scales,

and should not have more than 20% of missing data. Finally, the magnetic compressibility (expressed as the ratio between the power associated with intensity fluctuations and the total magnetic energy; Bavassano et al. 1982) must not exceed 0.25 within the inertial range, which ensures that we avoid data samples containing strong transient events or shocks (which could alter the nature of the wave modes under investigation), and to ensure that the observed $k_\parallel$ fluctuations belong to unperturbed solar wind turbulence. It is worth noting that the data selection has been performed regardless of wind type so that we could identify as many time intervals as possible and to explore the possible link between large-scale and small-scale features of solar wind fluctuations irrespective of solar wind speed. This approach and criteria yield a statistical sample of $N = 278$ time intervals from 12 yr of *Wind* observations.

Figure 1 shows the time profiles of the solar wind bulk speed V, magnetic field intensity B, proton number density n_p, pitch angle θ_{VB}, proton temperature anisotropy $T_\perp/T_\parallel$, and parallel proton plasma beta $\beta_\parallel$ for a typical high-speed stream observed at the beginning of 2005. The red area highlights one of the selected time intervals, identified from 13:36:56 to 14:36:44 UT on 2005 January 3, when the average of the displayed solar wind parameters are $\langle V \rangle = 631 \, \mathrm{km \, s^{-1}}$, $\langle B \rangle = 6.43$ nT, $\langle n_p \rangle = 1.93$ cm^{-3}, $\langle \theta_{VB} \rangle = 10°$, $\langle T_\perp/T_\parallel \rangle = 2.9$, and $\langle \beta_\parallel \rangle = 0.13$.

3. Analysis Results

The resulting magnetic field data sets are used to evaluate the total magnetic energy spectrum, i.e., the trace of the spectral matrix, E_B, and the normalized magnetic helicity spectrum σ_m, which, according to Matthaeus et al. (1982) and Matthaeus & Goldstein (1982), can be expressed as

$$\sigma_m(\omega) = \frac{2 \, \mathrm{Im}[Y^*(\omega) \cdot Z(\omega)]}{E_B}, \qquad (1)$$

where ω is the frequency, Y and Z are the Fourier transforms of the y and z magnetic field components in the Geocentric Solar Ecliptic coordinate system, and $*$ indicates the complex conjugate. The parameter σ_m is a measure of the polarization of the magnetic fluctuations in their wave-like representation: it is equal to 0 for plane-polarized waves and to ± 1 for right- and left-handed circularly polarized waves. However, the sign of the normalized magnetic helicity strictly depends on the orientation of the background magnetic field. Indeed, for left-handed polarized waves the magnetic helicity is positive (negative) in outward (inward) magnetic sectors. In order to properly relate the magnetic helicity sign to the intrinsic wave polarization, the magnetic field direction has been reversed whenever the measurements have been carried out in outward magnetic sectors. It transpires that a left-handed polarized wave will always return a positive magnetic helicity value.

The σ_m and E_B spectra for the data sample of Figure 1 are shown in Figure 2. While the normalized magnetic helicity is on average approximately zero within the inertial range (as is well known since magnetic helicity spectra were first evaluated in the solar wind; Matthaeus & Goldstein 1982; Goldstein et al. 1994), σ_m clearly exhibits a coherent bump near the proton gyrofrequency in the spacecraft frame, which is $\Omega_{p,\mathrm{SC}} \sim 0.6$ Hz in the solar wind sample under examination. Since the examined field-aligned time intervals are populated
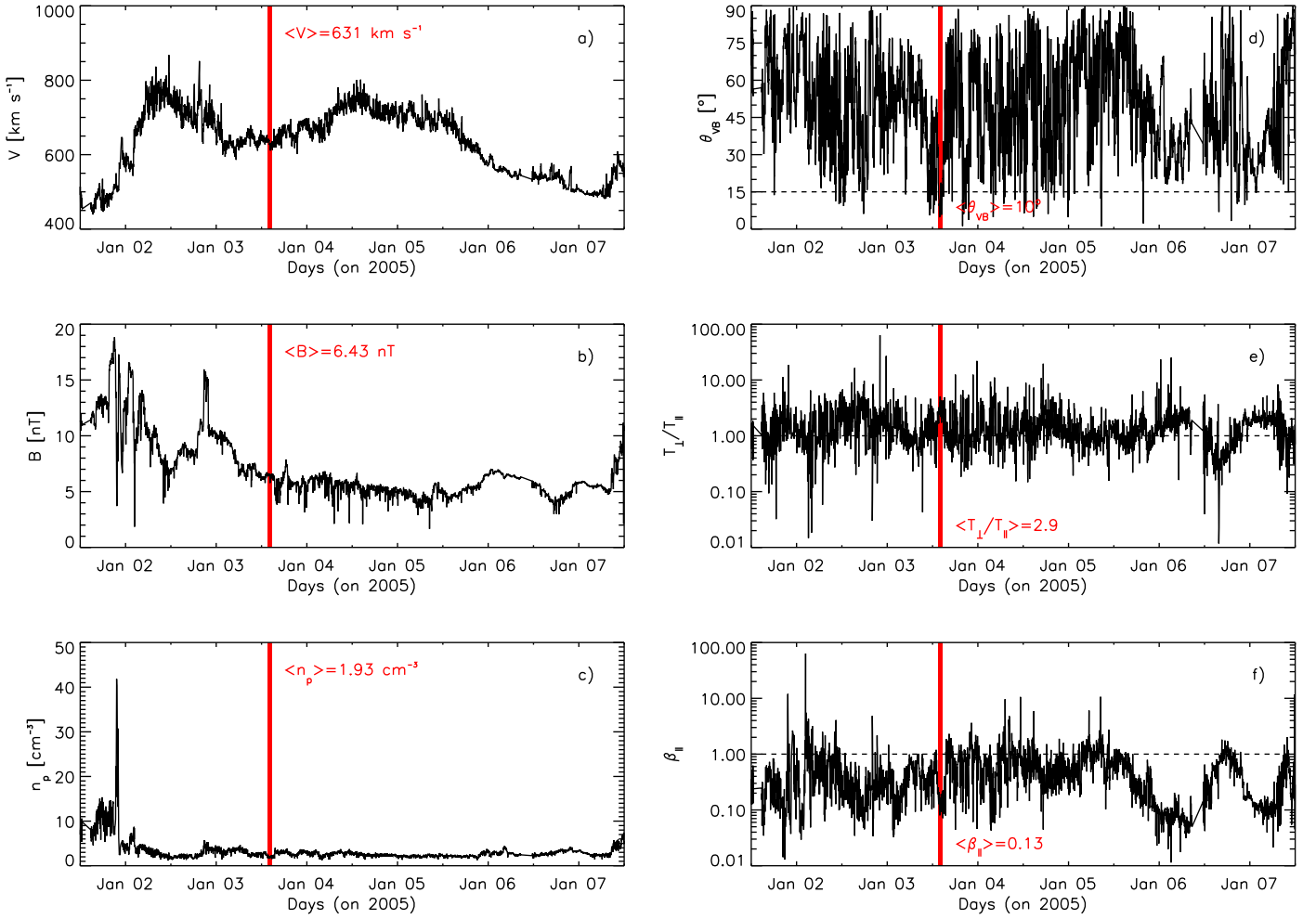
Figure 1. Time profiles of solar wind bulk speed (a), magnetic field intensity (b), proton number density (c), angle between the velocity and magnetic field vectors (d), proton temperature anisotropy (e), and parallel proton plasma beta (e) from noon on 2005 January 1 to noon of 2005 January 7; the average of the solar wind parameters relative to one of the selected time intervals (red area) is reported in each panel; the dashed line in (d) represents the threshold of 15° for the degree of alignment imposed while selecting the time intervals; the dashed lines in (e) and (f) refer to temperature isotropy and plasma–magnetic pressure balance, respectively.

mostly by $k_\parallel$ fluctuations, the peak in the σ_m spectrum is a robust signature of the presence of parallel-propagating left-handed polarized ICWs. The integral of the normalized magnetic helicity spectrum over the frequency range around the observed peak (gray area) can be considered a measure of the intensity of ICWs and, in turn, of the efficiency of their generation mechanism. In this time interval, the integral is $\hat{\sigma}_m = 0.71$.

Quite interestingly, corresponding to the peaks in the σ_m spectrum at $\omega \sim \Omega_{p,SC}$ and also at $\omega \sim 0.2\,\mathrm{Hz}$ are power enhancements in the total magnetic energy spectrum E_B. This is further evidence for the presence of ICWs in the analyzed data sample (Jian et al. 2009, 2010; Gary et al. 2016). However, in order to study how the existence of ICWs at proton scales is related to the amplitude of the turbulent fluctuations (as suggested by Telloni & Bruno 2016), we should estimate the total power in the magnetic fluctuations in the inertial range, for instance between 0.01 and 0.1 Hz (gray area), where the spectrum clearly exhibits a Kolmogorov-like $-5/3$ scaling. For this time interval, the integral of E_B over the 0.01–0.1 Hz frequency band is $W = 7.5 \times 10^{-2}\,\mathrm{nT}^2$.

The normalized magnetic helicity $\hat{\sigma}_m$ at frequencies around $\Omega_{p,SC}$, the power level of the magnetic fluctuations W at fluid scales (in the 0.01–0.1 Hz frequency range, which has been

checked to fall within the inertial range for all the studied samples), and the averages of the temperature anisotropy $T_\perp/T_\parallel$, solar wind speed V, and parallel plasma beta $\beta_\parallel$ are estimated for all the 278 selected time intervals. These quantities are shown in the color-coded scatterplots of Figure 3 (the marked circle refers to the data sample of Figure 1), where the color saturation from blue to red corresponds to the increasing density of cases (defined by counting how many data points fall within an arbitrary fixed squared area centered on each measure). This will enable us to relate fluid and kinetic parameters of solar wind $k_\parallel$ fluctuations that are possibly associated with ICWs.

Panel (a) of Figure 3 displays the distribution of the magnetic energy in the inertial range W (normalized to the lowest value obtained throughout the analysis, W_0) as a function of $T_\perp/T_\parallel$. Panels (b)–(d) show how the values assumed by $\hat{\sigma}_m$ at proton scales are related to V, W/W_0 and $T_\perp/T_\parallel$, respectively. Finally, panel (e) represents the observations in the $\beta_\parallel - T_\perp/T_\parallel$ space, where the different lines correspond to different plasma instabilities (as adapted from Hellinger et al. 2006, for a maximum growth rate $\gamma \sim 10^{-3}\Omega_p$). As shown by the Spearman's rank correlation coefficient ρ (green dashed lines) some degree of correlation is observed among all the parameters under investigation. In particular, the inverse
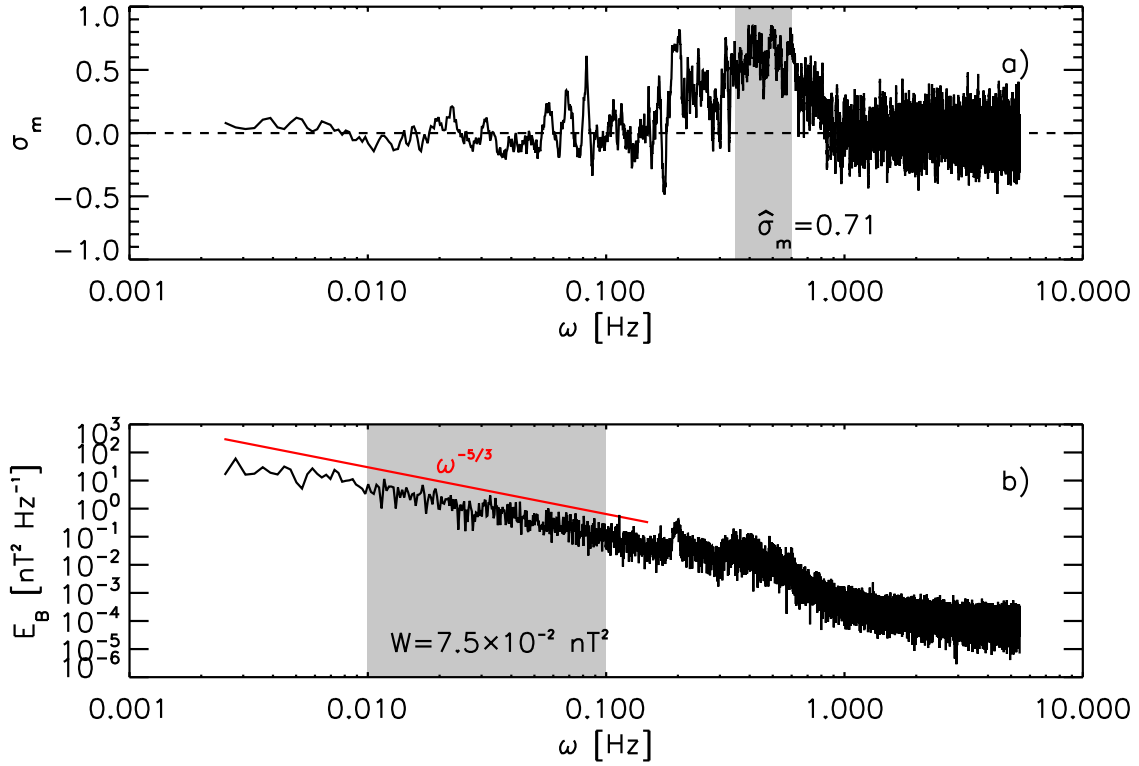
Figure 2. Spectrum of the normalized magnetic helicity σ_m (a) and total magnetic energy E_B (b); the gray areas highlight the frequency bands where σ_m and E_B are integrated: the corresponding values are reported in each panel; the dashed line in (a) refers to lack of coherence in $\boldsymbol{B_0}$; a linear $-5/3$ scaling is shown for reference in (b).

correlation exhibited by the proton parallel plasma beta $\beta_{\parallel}$ and the temperature anisotropy $T_{\perp}/T_{\parallel}$ confirms the existence of such a relation, shown for the first time by Marsch et al. (2004) for core protons in high-speed streams, also in the field-aligned solar wind turbulence. To test whether the observed correlations might have arisen by chance, the Student's t-test has been performed. For $N - 2 = 276$ degrees of freedom, a significance level $P < 0.001$ is always obtained, indicating that the correlation coefficients may be regarded as highly significant.

The results reported in Figure 3 robustly indicate that there exists a link between fluid and kinetic parameters during time intervals populated by ICWs. Correlation is found between the power level of the magnetic fluctuations within the inertial range and the temperature anisotropy (panel (a) of Figure 3). A high total magnetic energy at fluid scales affects the plasma at kinetic scales, inducing the proton VDF to deviate from a Maxwellian distribution, becoming instead highly anisotropic. Correlations are found also between the polarization of the magnetic fluctuations at proton scales and both the temperature anisotropy (panel (c) of Figure 3) and the amplitude of the turbulent fluctuations (panel (b) of Figure 3). Recalling that the value of $\hat{\sigma}_m$ at $\omega \sim \Omega_{p,\mathrm{SC}}$ can be considered a proxy for the number of ICWs present in the solar wind plasma, it indicates that as magnetic fluctuations become more and more energetic at large scales, more and more ICWs are identified at proton scales. In other words, the existence of ICWs might well be due to the presence of strong Alfvénic fluctuations within the inertial range. Regarding the distribution of the bulk speed as a function of $\hat{\sigma}_m$, large values of normalized magnetic helicity are found both in fast and slow solar wind, even if high-speed streams ($V \gtrsim 500\,\mathrm{km\,s^{-1}}$) are always characterized by larger magnetic helicity ($\hat{\sigma}_m \gtrsim 0.4$) at the proton gyrofrequency in the

spacecraft frame (panel (b) of Figure 3). This indicates that the critical parameter in regulating the presence of ICWs is not the wind speed, rather the power associated with the magnetic fluctuations within the inertial range. Indeed, while the fast wind is always populated by large-amplitude Alfvénic fluctuations, only a particular class of slow wind, the so-called Alfvénic slow wind, carries magnetic fluctuations with amplitudes as large as those advected by high-speed streams (e.g., D'Amicis & Bruno 2015). Finally, ICWs are found to occupy a region of the $\beta_{\parallel} - T_{\perp}/T_{\parallel}$ space that is close to the marginal stability condition for the proton cyclotron instability (panel (e) of Figure 3), where $T_{\perp} > T_{\parallel}$ and $\beta_{\parallel} < 1$.

4. Discussion and Conclusions

Solar wind turbulence may be described as the combination of a magnetic field background spectrum, common to both high- and low-speed streams (Bruno et al. 2017), and a turbulent large-amplitude Alfvénic spectrum, characteristic of the fast solar wind, on which it is superposed. The larger the power associated with the Alfvénic fluctuations within the inertial range, the steeper the slope of the spectrum at proton scales, beyond the high-frequency break separating fluid from kinetic scales (Bruno et al. 2014).

In this context and from the results outlined in the previous section it is possible to arrive at the following scenario. The high-frequency part of the turbulent Alfvénic fluctuations interacts with protons at frequencies near Ω_p, via resonant ion cyclotron scattering, releasing energy across the magnetic field. This heats protons in a direction perpendicular to the magnetic field, leading the VDFs becoming anisotropic. The degree of temperature anisotropy would thus be related to the amplitude of the magnetic fluctuations within the inertial range, as
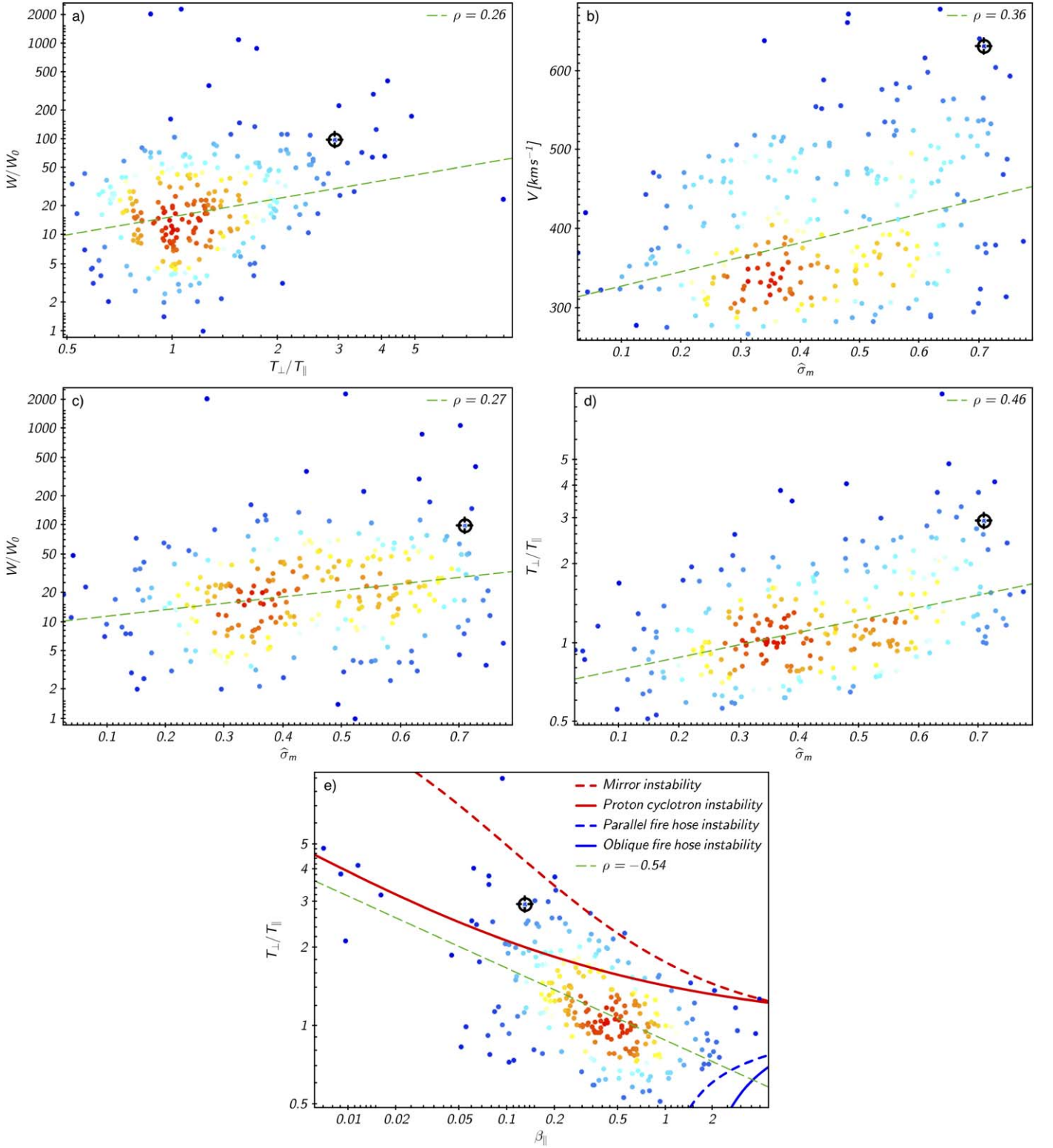
Figure 3. Color-coded scatterplots of W/W_0 vs. $T_\perp/T_\parallel$ (a), V vs. $\hat{\sigma}_m$ (b), W/W_0 vs. $\hat{\sigma}_m$ (c), $T_\perp/T_\parallel$ vs. $\hat{\sigma}_m$ (d) and $T_\perp/T_\parallel$ vs. $\beta_\parallel$ (e); colors from blue to red correspond to the increasing density of observations (see the text); the corresponding Spearman's rank correlation coefficient ρ (represented by the green dashed line) is reported in each panel; the marked circle refers to the data sample of Figure 1; different plasma instabilities are marked in the $\beta_\parallel - T_\perp/T_\parallel$ space with different line types as listed in the panel legend.

confirmed by the correlation observed between $T_\perp/T_\parallel$ and the magnetic energy at fluid scales W (panel (a) of Figure 3). With the strong departure from an isotropic, thermal equilibrium, plasma instabilities develop to release the excess of

(perpendicular) energy via the generation of waves. The subsequent enhanced scattering of charged particles then reduces the anisotropy of the particle VDFs. For $T_\perp/T_\parallel > 1$ the cyclotron instability develops (e.g., Gary et al. 1994),

driving the formation of ICWs at frequencies near the proton gyrofrequency. The observational evidence that the signature of the ICWs, namely, a high value of $\hat{\sigma}_m$ around $\Omega_{p,\mathrm{SC}}$, is correlated with higher power levels of turbulent fluctuations and to larger temperature anisotropies (panels (b) and (c) of Figure 3), corroborates the interpretation that ICWs are modes driven by the proton cyclotron instability and that there must be some response of the generation mechanism to the level of the energy transfer rate along the inertial range. In other words, when more energy is built up in the anisotropic VDFs, the mechanism underlying the formation of the ICWs should be more efficient, driving the generation of a larger number of waves. This hypothesis is supported by the statistical results shown in the previous section.

As a final concluding remark, although this work provides strong observational evidence for a generation of ICWs driven by thermal anisotropy, it is worth noting that it cannot be excluded the opposite interpretation, namely, that it might be the dissipation of ICWs to lead the proton VDFs out of the thermal equilibrium. For instance, on the basis of a novel approach for measuring the dissipation rate spectrum at proton scales, He et al. (2019) have recently provided robust hints that ICWs are dissipated in the magnetosheath turbulence, driving the proton temperature distribution to become anisotropic. Thus, such a wave–particle interaction process might also be at work in the solar wind turbulence, even if it cannot be observationally proved, due to the measurement limitations. However, indirect evidence for the dissipation of ICWs in the solar wind turbulence has been provided by Duan et al. (2018). Indeed, the spectral steepening of the $k_\parallel$ fluctuations observed beyond the proton cyclotron resonance frequency has been interpreted as a clear signature of the dissipation of ICWs. The dissipation and excitations of ICWs are likely at work at the same time and scales in the solar wind turbulence, and only the advent of the upcoming *Solar Orbiter* mission will solve this topic.

ORCID iDs

Daniele Telloni https://orcid.org/0000-0002-6710-8142
Francesco Carbone https://orcid.org/0000-0002-3559-5273
Roberto Bruno https://orcid.org/0000-0002-2152-0115
Gary P. Zank https://orcid.org/0000-0002-4642-6192
Luca Sorriso-Valvo https://orcid.org/0000-0002-5981-7758
Salvatore Mancuso https://orcid.org/0000-0002-9874-2234

References

Antonucci, E. 2006, SSRv, 124, 35
Antonucci, E., Abbo, L., & Telloni, D. 2012, SSRv, 172, 5
Bale, S. D., Kasper, J. C., Howes, G. G., et al. 2009, PhRvL, 103, 211101
Bavassano, B., Dobrowolny, M., Fanfoni, G., Mariani, F., & Ness, N. F. 1982, SoPh, 78, 373
Bourouaine, S., Marsch, E., & Neubauer, F. M. 2010, GeoRL, 37, 14104
Bruno, R., & Telloni, D. 2015, ApJL, 811, L17
Bruno, R., Telloni, D., DeIure, D., & Pietropaolo, E. 2017, MNRAS, 472, 1052
Bruno, R., Trenchi, L., & Telloni, D. 2014, ApJL, 793, L15
Cranmer, S. R., Kohl, J. L., Noci, G., et al. 1999, ApJ, 511, 481
D'Amicis, R., & Bruno, R. 2015, ApJ, 805, 84
Duan, D., He, J., Pei, Z., et al. 2018, ApJ, 865, 89
Gary, S. P., Jian, L. K., Broiles, T. W., et al. 2016, JGRA, 121, 30
Gary, S. P., McKean, M. E., Winske, D., et al. 1994, JGR, 99, 5903
Goldstein, M. L., Roberts, D. A., & Fitch, C. A. 1994, JGR, 99, 11519
He, J., Duan, D., Wang, T., et al. 2019, ApJ, 880, 121
He, J., Marsch, E., Tu, C., Yao, S., & Tian, H. 2011, ApJ, 731, 85
He, J., Wang, L., Tu, C., Marsch, E., & Zong, Q. 2015, ApJL, 800, L31
Hellinger, P., Trávníček, P., Kasper, J. C., & Lazarus, A. J. 2006, GeoRL, 33, L09101
Jian, L. K., Russell, C. T., Luhmann, J. G., et al. 2009, ApJL, 701, L105
Jian, L. K., Russell, C. T., Luhmann, J. G., et al. 2010, JGRA, 115, A12115
Kohl, J. L., Noci, G., Antonucci, E., et al. 1998, ApJL, 501, L127
Kohl, J. L., Noci, G., Cranmer, S. R., & Raymond, J. C. 2006, A&ARv, 13, 31
Lepping, R. P., Acūna, M. H., Burlaga, L. F., et al. 1995, SSRv, 71, 207
Marsch, E. 2006, LRSP, 3, 1
Marsch, E., Ao, X. Z., & Tu, C. Y. 2004, JGR, 109, A04102
Marsch, E., Schwenn, R., Rosenbauer, H., et al. 1982, JGR, 87, 52
Matthaeus, W. H., & Goldstein, M. L. 1982, JGR, 87, 6011
Matthaeus, W. H., Goldstein, M. L., & Smith, C. 1982, PhRvL, 48, 1256
Ogilvie, K., Chornay, D., Fritzenreiter, R., et al. 1995, SSRv, 71, 55
Podesta, J. J., & Gary, S. P. 2011, ApJ, 734, 15
Telloni, D., & Bruno, R. 2016, MNRAS, 463, L79
Telloni, D., Bruno, R., & Trenchi, L. 2015, ApJ, 805, 46
Woodham, L. D., Wicks, R. T., Verscharen, D., & Owen, C. J. 2018, ApJ, 856, 49
Zhao, G. Q., Feng, H. Q., Wu, D. J., Pi, G., & Huang, J. 2019, ApJ, 871, 175

---

8   https://cdaweb.sci.gsfc.nasa.gov/index.html